signals

MDPI

Article

Hybrid Chirp Signal Design for Improved Long-Range (LoRa) Communications

Md. Noor-A-Rahim [1,*], M. Omar Khyam [2], Apel Mahmud [3], Xinde Li [4], Dirk Pesch [1] and H. Vincent Poor [5]

1 School of Computer Science & IT, University College Cork, T12 K8AF Cork, Ireland; d.pesch@cs.ucc.ie
2 School of Engineering and Technology, Central Queensland University, Melbourne, QLD 4701, Australia; m.khyam@cqu.edu.au
3 Faculty of Engineering and Environment, Northumbria University Newcastle, Newcastle upon Tyne NE7 7YT, UK; md.a.mahmud@northumbria.ac.uk
4 School of Automation, Southeast University, Nanjing 210096, China; xindeli@seu.edu.cn
5 Department of Electrical and Computer Engineering, Princeton University, Princeton, NJ 08544, USA; poor@princeton.edu
* Correspondence: m.rahim@cs.ucc.ie

Abstract: Long-range (LoRa) communication has attracted much attention recently due to its utility for many Internet of Things applications. However, one of the key problems of LoRa technology is that it is vulnerable to noise/interference due to the use of only up-chirp signals during modulation. In this paper, to solve this problem, unlike the conventional LoRa modulation scheme, we propose a modulation scheme for LoRa communication based on joint up- and down-chirps. A fast Fourier transform (FFT)-based demodulation scheme is devised to detect modulated symbols. To further improve the demodulation performance, a hybrid demodulation scheme, comprised of FFT- and correlation-based demodulation, is also proposed. The performance of the proposed scheme is evaluated through extensive simulation results. Compared to the conventional LoRa modulation scheme, we show that the proposed scheme exhibits over 3 dB performance gain at a bit error rate of 10^{-4}.

Keywords: LoRa; LoRaWAN; IoT; LPWAN; chirp modulation

Citation: Noor-A-Rahim, M.; Khyam, M.O.; Mahmud, A.; Li, X.; Pesch, D.; Poor, H.V. Hybrid Chirp Signal Design for Improved Long-Range (LoRa) Communications. *Signals* **2022**, *3*, 1–10. https://doi.org/10.3390/signals3010001

Academic Editor: Chin-Ling Chen

Received: 25 November 2021
Accepted: 23 December 2021
Published: 5 January 2022

1. Introduction

The Internet of Things (IoT) has become the key technology to connect the physical world with the cyber world. The IoT now connects billions of devices embedded into the physical world to the Internet and allows us to share the data generated by them. Low-power wide-area (LPWA) technologies are one of the key machine-type communications (MTC) technologies enabling IoT networks with low energy consumption and reasonable reliability. In recent years, a number of LPWA network (LPWAN) technologies have been proposed, including Sigfox, Narrow-Band IoT (NB-IoT), and LoRa, to name a few [1]. Of them, LoRa has attracted much attention because of its openness and flexibility, which has led to exceptional commercial growth of LoRa-based offerings among the evolving LPWANs [2]. Furthermore, LoRa offers several benefits over conventional communication schemes thanks to its chirp spread spectrum modulation technique, which includes a constant signal envelope, energy-efficient long-range communication, robustness against narrow-band interference, and Doppler effect [3]. Despite its advantages, interference poses a significant problem for LoRa modulation, as it uses ISM bands; a number of other wireless technologies share the same spectrum [4]. In this light, the co-existence of both LoRaWAN or other LPWA networks has been studied extensively in recent years. For example, coded [5] or independent [6] message replications through time diversity have been proposed for both LoRaWAN or other LPWA networks. The co-existence of LoRa with Sigfox and IEEE 802.15.4 g has also been studied in [7,8], respectively.

Since LoRa is popular technology, multiple independent LoRa networks are expected to be used in close vicinity. Therefore, LoRa signals are also vulnerable to the same spreading factor interference, particularly for large-scale LoRa IoT deployments. The demodulation of LoRa under such a condition (known as capture effect) has been analyzed with mathematical models in [9]. Spreading factor allocation strategies have been used to enhance LoRa capacity in [10]. The physical layer of LoRa has been modeled mathematically in [11], while a closed-form approximation of LoRa modulation BER performance is presented in [7].

Despite significant efforts towards mitigating noise/interference effects on LoRa-based systems, interference still poses a significant problem for LoRa modulation. The technical reason behind the noise/interference in the LoRa modulation scheme is it uses either up-or down-chirp as a basis to encode data in a cyclic manner, where a chirp is divided into two sub-chirps (Figure 1). As a result, when the symbol value (k) increases, the bandwidth of the first sub-chirp decreases (Figure 1). In this situation, when demodulation is performed, the strength of the demodulated signal becomes weaker [12]. Therefore, in the presence of the interference/noise, a false peak is detected. A detailed description of LoRa demodulation is given in Section 2.

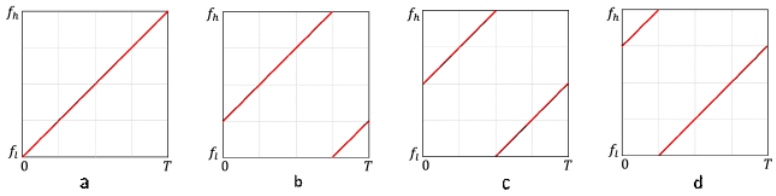

Figure 1. Time-frequency representation of traditional LoRa modulation for $\mathcal{S} = 2$. (**a**) $k = 0$, (**b**) $k = 1$, (**c**) $k = 2$, (**d**) $k = 3$.

In this paper, we propose a modulation scheme for LoRa communication based on joint up- and down-chirps to solve this problem. The proposed system is inspired by the ultrasonic indoor positioning systems proposed in [12,13], which demonstrated that a system that uses both up- and down-chirps at the same time is more resilient against noise/interference. The advantage of the proposed modulation scheme is that the bandwidth of the sub-chirps within a chirp does not reduce significantly with a higher symbol value (e.g., Figure 2d) compared to the conventional design (e.g., Figure 1d).

To demodulate symbols in the proposed scheme, we propose a fast Fourier transform (FFT)-based demodulation scheme and develop a hybrid demodulation scheme for further enhancing the demodulation performance. We show that the proposed scheme significantly outperforms the conventional LoRa modulation scheme with and without interference scenarios. Thus, the novelty and contributions of this paper can be summarized as follows:

- A joint up- and down-chirp-based modulation scheme which is more resilient against noise/interference is proposed;
- A hybrid demodulation scheme to enhance demodulation performance is proposed;
- The proposed techniques are validated through simulations for different scenarios.

The remainder of the paper is organized as follows. In Section 2, a brief literature review on LoRa performance enhancement is described. In Section 3, we briefly present the modulation and demodulation strategies for traditional LoRa communication. The proposed and enhanced modulation schemes are presented in Section 4. The performance of the proposed schemes is presented and compared in Section 5. Finally, we conclude in Section 6.

2. Related Work

Enhancing LoRa performance is challenging in the presence of noise/interference. In [10], spreading factor allocation strategies were used to enhance LoRa capacity, whereas in [14], different MAC layer techniques were used. Furthermore, in [15], the density of

LoRa gateways was increased to improve the LoRa capacity. Research on the LoRa physical layer has also been conducted to improve the LoRa performance. For instance, in [16], capture effect and successive interference cancellation were considered to represent LoRa capacity. In [17], a combination of CSS and on-off keying was used to transmit LoRa signals simultaneously. In [18], chirp spread spectrum (CSS) modulation was compared with a binary phase-shift keying (BPSK); the results showed that CSS is more robust against interference compared to BPSK. To enhance LoRa capacity, error correction schemes were used in [19], whereas [20] used interleaved chirp spreading. In [21], the co-existence of LoRa and interleaved chirp spreading was investigated.

3. Preliminaries

3.1. LoRa Modulation

Chirp spread spectrum modulation is used in LoRaWAN to generate the LoRa signal. In LoRa modulation, S bits are mapped into a LoRa modulated symbol, where $\mathcal{S}$ is the spreading factor. Hence, we need to create $2^{\mathcal{S}}$ symbols to accommodate all possible bit combinations. The time-domain LoRa signal for one symbol period can be written as [22]:

$$x_k(t) = \begin{cases} Ae^{j2\pi\left((f_l+\frac{kB}{2^{\mathcal{S}}})t+\frac{Bt^2}{2T}\right)} & \text{if } t \leq \tau \\ Ae^{j2\pi\left((f_l+\frac{kB}{2^{\mathcal{S}}}-B)t+\frac{Bt^2}{2T}\right)} & \text{if } t > \tau \end{cases} \tag{1}$$

where $k \in \{0, 2^{\mathcal{S}} - 1\}$ is the decimal representation of $\mathcal{S}$ bits (if $\boldsymbol{b}_k$ is the bits of the current LoRa symbol to be transmitted, then k can be defined as $k = \sum_{i=1}^{\mathcal{S}} \boldsymbol{b}_k(i) \cdot 2^{i-1}$, where i represents the index of the bits). In (1), A and T represent the amplitude and symbol duration of one LoRa signal, respectively. The bandwidth B of the LoRa signal is defined by $B = f_h - f_l$, where f_h and f_l are the maximum and minimum frequencies, respectively. Each LoRa modulated symbol satisfies the time-bandwidth constraint $BT = 2^{\mathcal{S}}$. The time of frequency hopping in one LoRa symbol period τ is defined by $\tau = T - \frac{kT}{2^{\mathcal{S}}}$. The spreading factor establishes a trade-off between the data rate and coverage range. The instantaneous frequency of $x_k(t)$ can be calculated as:

$$f_{x_k}(t) = \begin{cases} f_l + \frac{kB}{2^{\mathcal{S}}} + \frac{B}{T}t & \text{if } t \leq \tau \\ f_l + \frac{kB}{2^{\mathcal{S}}} - B + \frac{B}{T}t & \text{if } t > \tau \end{cases} \tag{2}$$

A simple example of the traditional LoRa modulation scheme is presented in Figure 1 for $\mathcal{S} = 2$, where each k represents a different bit.

3.2. LoRa Demodulation

The received signal in the presence of interference and noise is given by:

$$y_k(t) = x_k(t) + \bar{x}_k(t) + w(t), \tag{3}$$

where $\bar{x}_k(t)$ is an interference signal (with a spreading factor the same as, or different than, $x_k(t)$ and $w(t)$ represents the complex white Gaussian noise with zero mean and variance σ_n^2. The demodulation of a received LoRa signal is generally performed either through matched filtering or de-chirping. In the former, the received signal is cross-correlated with all possible combinations of the signature signals. A high correlation peak implies that the desired signature signal is presented within the received signal and the index of the peak denotes the starting of the desired signature signal, which is also useful to determine the range information between the transmitter and receiver. Although this approach has several advantages, including high range resolution and enhanced SNR [23], the major problem of this approach is its high computational complexity.

The underlying principle of the latter case involves multiplying the received signal with a synchronized raw down-chirp having the same $\mathcal{S}$ and B. Assuming no noise and interference, the multiplied signal becomes:

$$z_k(t) = x_k(t) \times Ae^{j2\pi\left(f_h t - \frac{Bt^2}{2T}\right)}, \tag{4}$$

where the second term in the multiplication represents the raw down-chirp signal. The instantaneous frequency of the multiplied signal can be given as follows:

$$f_{z_k}(t) = \begin{cases} f_l + f_h + \frac{kB}{2^{\mathcal{S}}} & \text{if } t \leq \tau \\ f_l + f_h + \frac{kB}{2^{\mathcal{S}}} - B & \text{if } t > \tau \end{cases} \tag{5}$$

Equation (5) implies that the demodulated signal comprises two intervals, where each consists of a constant frequency. In both intervals, the frequency linearly depends on the offset, and the difference between the levels is B. Now, suppose the signal is down-sampled at the rate of B Hz. In that case, the instantaneous frequency turns into a continuous frequency over the entire chirp and, after subtracting the term $f_l + f_h$, is proportional to the shift k. As a result, the resultant sampled signal becomes a pure sinusoid. When FFT is performed on that sinusoid, a flat response is obtained with the peak shifted by the k value [15]. The above process can be summarized by the following equation:

$$\hat{k} = \text{argmax}\, \mathcal{F}(z_k(t)) - f_l - f_h \tag{6}$$

where $\hat{k}$ is an estimate of the transmitted symbol's index k and $\mathcal{F}(z_k(t))$ gives the frequency domain representation after performing down-sampling on $z_k(t)$ at the rate of B Hz. More details on the down-sampling and frequency domain representation can be found in [24].

4. Proposed Modulation Scheme

In previous studies, it was shown that the chirp signal design based on joint up and down chirps always exhibits better performance compared to the chirp signal composed of either only up- or down-chirps. For example, in the context of indoor positioning, the scheme based on joint up- and down-chirps provides better location accuracy than the one based on only either up- or down-chirp schemes. Motivated by this, we propose a LoRa modulation scheme using both up- and down-chirps in contrast to the conventional either up- or down-chirp approach. In our proposed scheme, we represent the first half of the $2^{\mathcal{S}}$ bit combinations with up-chirp based signals, while the rest of the combinations are represented by down-chirp based signals. With the proposed scheme, the instantaneous frequency of $k^{th} \in \{0, 2^{\mathcal{S}} - 1\}$ symbol is given by

$$f_{x_k}(t) = \begin{cases} f_l + \frac{kB}{2^{\mathcal{S}-1}} + \frac{B}{T}t & \text{if } t \leq \tau_{k_u} \text{ and } k < 2^{\mathcal{S}-1} \\ f_l + \frac{kB}{2^{\mathcal{S}-1}} - B + \frac{B}{T}t & \text{if } t > \tau_{k_u} \text{ and } k < 2^{\mathcal{S}-1} \\ f_h - \frac{\kappa B}{2^{\mathcal{S}-1}} - \frac{B}{T}t & \text{if } t \leq \tau_{k_d} \text{ and } k \geq 2^{\mathcal{S}-1} \\ f_h - \frac{\kappa B}{2^{\mathcal{S}-1}} + B - \frac{B}{T}t & \text{if } t > \tau_{k_d} \text{ and } k \geq 2^{\mathcal{S}-1}, \end{cases} \tag{7}$$

where $\kappa = mod(k, 2^{\mathcal{S}-1})$, $\tau_{k_u} = T - \frac{kT}{2^{\mathcal{S}-1}}$, and $\tau_{k_d} = T - \frac{\kappa T}{2^{\mathcal{S}-1}}$. With the above specifications, a simple example of the proposed LoRa modulation (for $\mathcal{S} = 2$) scheme is shown in Figure 2.

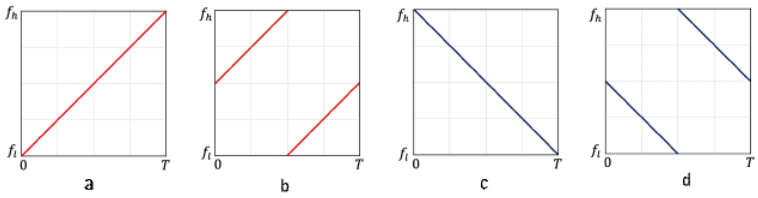

Figure 2. Time-frequency representation of the proposed LoRa modulation for $\mathcal{S} = 2$. (**a**) $k = 0$, (**b**) $k = 1$, (**c**) $k = 2$, (**d**) $k = 3$.

4.1. FFT-Based Demodulation

We propose an FFT-based demodulation technique for the up- and down-chirp-based LoRa modulation. At the receiver, the received signal is first multiplied by a synchronized raw down-chirp and then by a synchronized raw up-chirp signal. Let us assume that the received signal corresponds to an up-chirp-based transmitted symbol (i.e., $k < 2^{\mathcal{S}-1}$). In the absence of noise and interference, the received signal becomes:

$$y_k(t) = \begin{cases} Ae^{2\pi(f_l + \frac{kB}{2^{\mathcal{S}-1}} + \frac{B}{T}t)t} & \text{if } t \leq \tau_{k_u} \\ Ae^{2\pi(f_l + \frac{kB}{2^{\mathcal{S}-1}} - B + \frac{B}{T}t)t} & \text{if } t > \tau_{k_u} \end{cases} \tag{8}$$

When the received signal is multiplied by a synchronized raw up-chirp $Ae^{j2\pi\left(f_l t + \frac{Bt^2}{2T}\right)}$, the resultant signal becomes:

$$z_{k_u}(t) = \begin{cases} A^2e^{2\pi(2f_l + \frac{kB}{2^{\mathcal{S}-1}} + 2\frac{B}{T}t)t} & \text{if } t \leq \tau_{k_u} \\ A^2e^{2\pi(2f_l + \frac{kB}{2^{\mathcal{S}-1}} - B + 2\frac{B}{T}t)t} & \text{if } t > \tau_{k_u} \end{cases} \tag{9}$$

On the other hand, when the received signal is multiplied by a synchronized raw down-chirp, the frequency of the resultant signal becomes:

$$z_{k_d}(t) = \begin{cases} A^2e^{2\pi(f_l + f_h + \frac{kB}{2^{\mathcal{S}-1}})t} & \text{if } t \leq \tau_{k_u} \\ A^2e^{2\pi(f_l + f_h + \frac{kB}{2^{\mathcal{S}-1}} - B)t} & \text{if } t > \tau_{k_u} \end{cases} \tag{10}$$

By examining the peak of the frequency spectrum obtained from (9) and (10), one can determine that the received signal corresponds to an up-chirp-based transmitted signal. We observe that (10) is similar to the traditional demodulation scheme, where only two frequency components are observed (as described in Section 3.2), while (9) is composed of multiple frequency components, where the signal power is distributed among the frequency components. As a result, after FFT, the peak of the frequency spectrum obtained from (10) will be much higher than the peak of the frequency spectrum obtained from (9). Note that a similar phenomenon can be observed when the down-chirp-based received signal is multiplied by a synchronized raw down- and up-chirp, respectively. Mathematically, the process can be described in the following manner. Firstly, we find the estimates of the index ($\hat{k}_u$) of the up-chirp-based transmitted symbol and the corresponding amplitude ($F_{\hat{k}_u}$) by the following manner:

$$\begin{aligned} \hat{k}_u &= \text{argmax}\, \mathcal{F}(z_{k_u}(t)) - f_l - f_h \\ F_{\hat{k}_u} &= \max(\mathcal{F}(z_{k_u}(t))) \end{aligned} \tag{11}$$

Similarly, for the down-chirp-based transmitted symbol, we find the index ($\hat{k}_d$) and the corresponding amplitude ($F_{\hat{k}_d}$):

$$\begin{aligned} \hat{k}_d &= \text{argmax}\, \mathcal{F}(z_{k_d}(t)) - f_l - f_h \\ F_{\hat{k}_d} &= \max\big(\mathcal{F}(z_{k_d}(t))\big) \end{aligned} \tag{12}$$

The estimated index of the transmitted symbol is given by

$$\hat{k} = \underset{i \in \{\hat{k}_u, \hat{k}_d\}}{\text{argmax}}(F_i).$$

4.2. Hybrid Demodulation

In this section, we propose a hybrid demodulation algorithm to further improve the performance of the proposed FFT-based demodulator. In the presence of noise/interference, sometimes the FFT demodulator incorrectly detects the transmitted up-chirp (down-chirp)-based signal as a down-chirp (up-chirp)-based signal. To tackle this ambiguity, we perform two cross-correlation operations after performing the FFT-based demodulation, as cross-correlation-based demodulation provides optimum detection. After performing the multiplication of the received signal with raw down- and up-chirp signals, we find one up-chirp-based candidate transmitted LoRa symbol and one down-chirp-based candidate transmitted LoRa symbol. Then, we perform cross-correlation between the received signal and the candidate symbols, from where the best matched symbol is considered the transmitted symbol. The proposed hybrid demodulation scheme is summarized in Algorithm 1.

Algorithm 1 Hybrid Demodulation Technique

1: Find $z_{k_u}(t)$ and $z_{k_d}(t)$ from (9) and (10), respectively.
2: Following (11) and (12), find the estimates of the up- and down-chirp-based transmitted symbol's indexes, i.e., $\hat{k}_u$ and $\hat{k}_d$, respectively.
3: Perform cross-correlation (the closed-form expression for the cross-correlation can be found in [25]) between the received signal and the LoRa symbols with indexes $\hat{k}_u$ and $\hat{k}_d$ and find the absolute cross-correlation values $X_{k_u}(\ell)$ and $X_{k_u}(\ell)$, respectively.

$$\begin{aligned} X_{\hat{k}_u}(\ell) &= \left| \int_{-\infty}^{\infty} y_k(t) \cdot x^*_{\hat{k}_u}(t-\ell) \right| \\ X_{\hat{k}_d}(\ell) &= \left| \int_{-\infty}^{\infty} y_k(t) \cdot x^*_{\hat{k}_d}(t-\ell) \right| \end{aligned}$$

4: Find the estimated index of the transmitted symbol by the following equation:

$$\hat{k} = \underset{i \in \{\hat{k}_u, \hat{k}_d\}}{\text{argmax}}(X_i[0])$$

The closed-form expression for the cross-correlation can be found in [25].

5. Numerical Results and Discussion

In this section, we present the performance evaluation of our proposed LoRa modulation and demodulation scheme. To evaluate the performance of our proposed scheme, a LoRa simulation environment was built in Matlab. The simulation parameters are summarized in Table 1. In the simulation, we set $B = 125$ KHz and a packet size of 200 bits. In Figure 3, we present the performance comparison between our proposed scheme and the traditional scheme in the presence of additive white Gaussian noise (AWGN). The bit error rate (BER) performance is presented for $\mathcal{S} = \{6, 8, 10\}$. As expected, the improved BER

performance is observed as $\mathcal{S}$ increases. We observe that the proposed LoRa modulation scheme outperforms the traditional LoRa modulation scheme for all scenarios. The proposed scheme exhibits over 3 dB improvement at a BER of 10^{-4} compared to the traditional scheme. A further improvement over the proposed FFT-based demodulation is observed by applying the proposed hybrid demodulation scheme, since the correlation performed in the hybrid demodulation eliminates the ambiguity in nature (up/down) of the received signal. For different spreading factors, in Table 2, we present the required signal-to-noise ratio (SNR) to obtain a packet error rate ≤ 0.01. For each case, we observe a significant improvement in the SNR threshold with our proposed modulation and demodulation schemes. The following examples demonstrate the significance of the above performance gain. Let us consider a LoRa system with operating frequency = 900 MHz, bandwidth = 125 kHz, transmission power = 2 dBm, and noise figure = 10 dBm. We calculate the received power based on the free space pathloss model [26]. With the conventional LoRa modulation scheme, one can achieve a communication range of 29 km and 58 km for $\mathcal{S} = 7$ and $\mathcal{S} = 9$, respectively, while meeting the packet error rate threshold of $\leq$0.01. On the other hand, our proposed modulation schemes can achieve a communication range of 52 km and 93 km for $\mathcal{S} = 7$ and $\mathcal{S} = 9$, respectively.

Table 1. Simulation Parameters.

Parameter	**Value**
Packet size	200 Bits
Bandwidth	125 kHz
Packet error rate threshold	0.01
Carrier frequency	915 MHz
Transmit power	2 dBm
Noise figure	10 dBm

Table 2. SNR (in dB) threshold comparison.

Sp. Fac / **Schemes**	$\mathcal{S} = 6$	$\mathcal{S} = 7$	$\mathcal{S} = 8$	$\mathcal{S} = 9$	$\mathcal{S} = 10$	$\mathcal{S} = 11$	$\mathcal{S} = 12$
Traditional	−3	−6	−9	−12	−15	−19	−22
Proposed (FFT)	−6	−11	−13	−16	−19	−22	−25
Proposed (Hybrid)	−8	−11	−14	−17	−19	−22	−26

Now, we present the performance of the proposed schemes in the presence of interference, where the desired LoRa signal collides with another LoRa signal. For interference signals with spreading factors $\mathcal{S} = \{6, 8, 10\}$, the BER performance comparison is presented in Figure 4. In the simulation, we set the noise as Gaussian distributed with variance $\sigma^2 = 1$. We consider the unit received power for the desired LoRa signal, while varyuing the received power of the interference LoRa signal to vary the signal-to-interference and noise ratio (SINR). Again, the BER performance improves as $\mathcal{S}$ increases, except in the scenario where the interference signal has the same spreading factor as the desired signal, for which the worst performance is observed. Similar to the results shown in Figure 3, we observe a performance improvement for all the scenarios with the proposed schemes. For all combinations of reference signals and interference signals, the SINR threshold comparison is presented in Table 3. Again, we find the minimum SINR required for each combination to achieve a packet error rate of 0.01. From the table, we observe that,

in most cases, the proposed schemes exhibit a better SINR threshold compared to the traditional scheme.

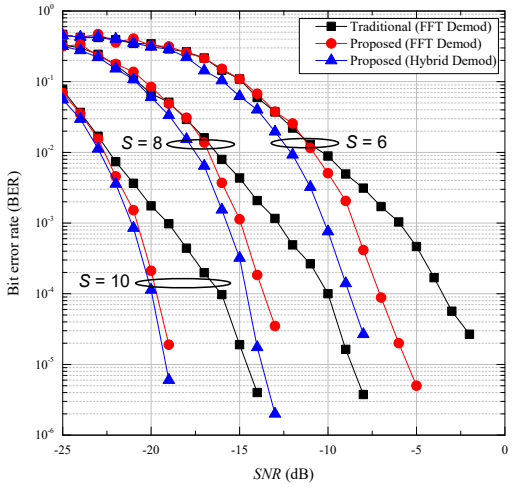

Figure 3. Performance comparison between the proposed and traditional LoRa modulation schemes with different spreading factors.

Table 3. SINR (in dB) threshold comparison. Traditional, proposed, and hybrid schemes are presented by green, blue, and red circles, respectively.

Int. / Des.	$\mathcal{S}=6$			$\mathcal{S}=7$			$\mathcal{S}=8$			$\mathcal{S}=9$			$\mathcal{S}=10$			$\mathcal{S}=11$			$\mathcal{S}=12$		
$\mathcal{S}=6$	0	0	0	−1	−2	−3	−1	−2	−3	−1	−2	−3	−1	−2	−4	−1	−3	−4	−1	−2	−4
$\mathcal{S}=7$	−3	−4	−5	0	0	0	−3	−5	−5	−3	−5	−6	−3	−5	−6	−3	−6	−6	−3	−6	−7
$\mathcal{S}=8$	−6	−7	−8	−5	−7	−8	0	0	0	−5	−7	−8	−6	−7	−8	−6	−7	−8	−6	−8	−9
$\mathcal{S}=9$	−10	−10	−10	−10	−10	−10	−8	−10	−10	0	−1	−1	−7	−11	−11	−8	−10	−11	−9	−10	−11
$\mathcal{S}=10$	−12	−12	−12	−12	−12	−13	−12	−12	−13	−11	−12	−13	0	0	−1	−10	−13	−14	−11	−13	−14
$\mathcal{S}=11$	−15	−15	−15	−15	−15	−15	−15	−15	−15	−15	−15	−16	−13	−15	−16	−1	−1	−1	−13	−16	−17
$\mathcal{S}=12$	−17	−17	−18	−17	−17	−17	−17	−18	−18	−18	−18	−18	−18	−18	−19	−17	−18	−18	−1	−1	−1

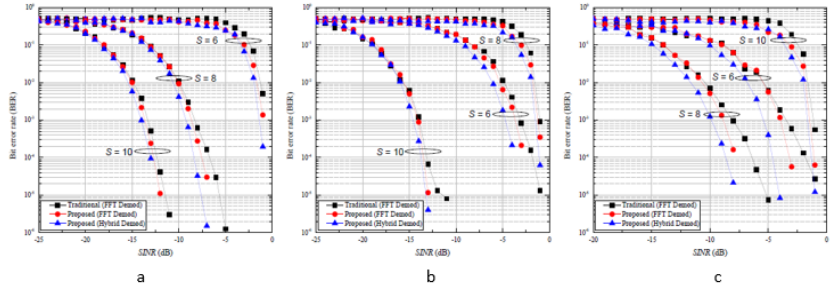

Figure 4. Performance comparison of different LoRa signals in the presence of interference. (**a**) Interference signal $\mathcal{S}=6$; (**b**) interference signal $\mathcal{S}=8$; (**c**) interference signal $\mathcal{S}=10$.

6. Conclusions

In this paper, we have proposed novel modulation and demodulation schemes for LoRa communications. The modulation scheme is designed based on up- and down-chirp

signals. An FFT-based demodulation scheme is proposed to detect the proposed modulated symbols. For further enhancement, a hybrid demodulation scheme is also presented, which is comprised of FFT- and correlation-based operations. With and without interference, the simulation results show that the proposed schemes exhibit better bit error rate performance compared to the conventional LoRa modulation scheme.

Author Contributions: Formal analysis, M.N.-A.-R. and M.O.K.; Investigation, A.M.; Methodology, M.O.K., A.M. and D.P.; Software, A.M. and X.L.; Supervision, D.P. and H.V.P.; Validation, X.L.; Writing–original draft, M.N.-A.-R.; Writing– review and editing, D.P. and H.V.P. All authors have read and agreed to the published version of the manuscript.

Funding: This publication has emanated from research conducted in part with the financial support of Science Foundation Ireland under Grant number 16/RC/3918. The work of H. V. Poor was supported in part by the U.S. National Science Foundation under Grant CCF-1908308.

Institutional Review Board Statement: Not applicable.

Informed Consent Statement: Not applicable.

Data Availability Statement: Not applicable.

Conflicts of Interest: The authors declare no conflict of interest.

References

1. Raza, U.; Kulkarni, P.; Sooriyabandara, M. Low Power Wide Area Networks: An Overview. *IEEE Commun. Surv. Tutor.* **2017**, *19*, 855–873. [CrossRef]
2. Sornin, N.; Luis, M.; Eirich, T.; Kramp, T.; Hersent, O. LoRaWAN specification. *LoRa Alliance* **2015**, *6*. Available online: https://www.scirp.org/(S(i43dyn45teexjx455qlt3d2q))/reference/ReferencesPapers.aspx?ReferenceID=1739358 (accessed on 1 December 2021).
3. Doroshkin, A.A.; Zadorozhny, A.M.; Kus, O.N.; Prokopyev, V.Y.; Prokopyev, Y.M. Experimental Study of LoRa Modulation Immunity to Doppler Effect in CubeSat Radio Communications. *IEEE Access* **2019**, *7*, 75721–75731. [CrossRef]
4. Ben Temim, M.A.; Ferré, G.; Laporte-Fauret, B.; Dallet, D.; Minger, B.; Fuché, L. An Enhanced Receiver to Decode Superposed LoRa-Like Signals. *IEEE Internet Things J.* **2020**, *7*, 7419–7431. [CrossRef]
5. Montejo-Sánchez, S.; Azurdia-Meza, C.A.; Souza, R.D.; Fernandez, E.M.G.; Soto, I.; Hoeller, A. Coded Redundant Message Transmission Schemes for Low-Power Wide Area IoT Applications. *IEEE Wirel. Commun. Lett.* **2019**, *8*, 584–587. [CrossRef]
6. Hoeller, A.; Souza, R.D.; Alcaraz López, O.L.; Alves, H.; de Noronha Neto, M.; Brante, G. Analysis and Performance Optimization of LoRa Networks With Time and Antenna Diversity. *IEEE Access* **2018**, *6*, 32820–32829. [CrossRef]
7. Reynders, B.; Meert, W.; Pollin, S. Range and coexistence analysis of long range unlicensed communication. In Proceedings of the 23rd International Conference on Telecommunications (ICT), Thessaloniki, Greece, 16–18 May 2016; pp. 1–6.
8. Orfanidis, C.; Feeney, L.M.; Jacobsson, M.; Gunningberg, P. Investigating interference between LoRa and IEEE 802.15.4g networks. In Proceedings of the IEEE 13th International Conference on Wireless and Mobile Computing, Networking and Communications (WiMob), Rome, Italy, 9–11 October 2017; pp. 1–8.
9. Bankov, D.; Khorov, E.; Lyakhov, A. Mathematical model of LoRaWAN channel access with capture effect. In Proceedings of the IEEE 28th Annual International Symposium on Personal, Indoor, and Mobile Radio Communications (PIMRC), Montreal, QC, Canada, 8–13 October 2017; pp. 1–5.
10. Cuomo, F.; Campo, M.; Caponi, A.; Bianchi, G.; Rossini, G.; Pisani, P. EXPLoRa: Extending the performance of LoRa by suitable spreading factor allocations. In Proceedings of the IEEE 13th International Conference on Wireless and Mobile Computing, Networking and Communications (WiMob), Rome, Italy, 9–11 October 2017; pp. 1–8.
11. Vangelista, L. Frequency Shift Chirp Modulation: The LoRa Modulation. *IEEE Signal Process. Lett.* **2017**, *24*, 1818–1821. [CrossRef]
12. Khyam, M.O.; Noor-A-Rahim, M.; Li, X.; Ritz, C.; Guan, Y.L.; Ge, S.S. Design of Chirp Waveforms for Multiple-Access Ultrasonic Indoor Positioning. *IEEE Sens. J.* **2018**, *18*, 6375–6390. [CrossRef]
13. Khyam, M.O.; Xinde, L.; Ge, S.S.; Pickering, M.R. Multiple Access Chirp-Based Ultrasonic Positioning. *IEEE Trans. Instrum. Meas.* **2017**, *66*, 3126–3137. [CrossRef]
14. Haxhibeqiri, J.; Moerman, I.; Hoebeke, J. Low Overhead Scheduling of LoRa Transmissions for Improved Scalability. *IEEE Internet Things J.* **2019**, *6*, 3097–3109. [CrossRef]
15. Croce, D.; Gucciardo, M.; Mangione, S.; Santaromita, G.; Tinnirello, I. LoRa Technology Demystified: From Link Behavior to Cell-Level Performance. *IEEE Trans. Wirel. Commun.* **2020**, *19*, 822–834. [CrossRef]
16. Noreen, U.; Clavier, L.; Bounceur, A. LoRa-like CSS-based PHY layer, Capture Effect and Serial Interference Cancellation. European Wireless 2018. In Proceedings of the 24th European Wireless Conference, Catania, Italy, 2–4 May 2018; pp. 1–6.

17. Hessar, M.; Najafi, A.; Gollakota, S. NetScatter: Enabling Large-Scale Backscatter Networks. In Proceedings of the 16th USENIX Symposium on Networked Systems Design and Implementation (NSDI 19), USENIX Association, Boston, MA, USA, 26–28 February 2019; pp. 271–284.
18. Reynders, B.; Pollin, S. Chirp spread spectrum as a modulation technique for long range communication. In Proceedings of the 2016 Symposium on Communications and Vehicular Technologies (SCVT), Mons, Belgium, 22 November 2016; pp. 1–5. [CrossRef]
19. Elshabrawy, T.; Robert, J. Enhancing LoRa Capacity using Non-Binary Single Parity Check Codes. In Proceedings of the 2018 14th International Conference on Wireless and Mobile Computing, Networking and Communications (WiMob), Limassol, Cyprus, 15–17 October 2018; pp. 1–7. [CrossRef]
20. Elshabrawy, T.; Robert, J. Interleaved Chirp Spreading LoRa-Based Modulation. *IEEE Internet Things J.* **2019**, *6*, 3855–3863. [CrossRef]
21. Edward, P.; Elzeiny, S.; Ashour, M.; Elshabrawy, T. On the Coexistence of LoRa- and Interleaved Chirp Spreading LoRa-Based Modulations. In Proceedings of the 2019 International Conference on Wireless and Mobile Computing, Networking and Communications (WiMob), Barcelona, Spain, 21–23 October 2019; pp. 1–6. [CrossRef]
22. Zhang, C.; Shi, J.; Zhang, Z.; Liu, Y.; Hu, X. FRFT-Based Interference Suppression for OFDM Systems in IoT Environment. *IEEE Commun. Lett.* **2019**, *23*, 2068–2072. [CrossRef]
23. Guo, Y.; Liu, Z. Time-Delay-Estimation-Liked Detection Algorithm for LoRa Signals Over Multipath Channels. *IEEE Wirel. Commun. Lett.* **2020**, *9*, 1093–1096. [CrossRef]
24. Ferré, G.; Giremus, A. LoRa Physical Layer Principle and Performance Analysis. In Proceedings of the IEEE International Conference on Electronics, Circuits and Systems (ICECS), Bordeaux, France, 9–12 December 2018; pp. 65–68. [CrossRef]
25. Chiani, M.; Elzanaty, A. On the LoRa Modulation for IoT: Waveform Properties and Spectral Analysis. *IEEE Internet Things J.* **2019**, *6*, 8463–8470. [CrossRef]
26. Rappaport, T.S. *Wireless Communications: Principles and Practice*; Prentice Hall: Hoboken, NJ, USA 1996.